



NONLINEAR DYNAMIC ANALYSIS OF BASE-ISOLATED FRAMES USING JULIA

Nguyen Xuan Thanh^{1*}

Abstract: Base isolation is a technique used in the field of structural passive control. In this technique, the superstructure is isolated from the ground motion by means of bearing systems. Thus, the transmission of the ground motion to superstructures is reduced. By “separating” the superstructure from its foundation, the input energy from the earthquake is mainly converted into the kinetic energy of the superstructure, only a small portion of it enters the superstructure in the form of strain energy, alleviating the damages to it. This article presents the modeling and the nonlinear dynamic analysis of base-isolated frame structures using linear theory (with non-classical damping matrix) and nonlinear theory (with 6-parameter Bouc-Wen bearing model). The computations are done with the aid from Julia scientific language. Results from case studies illustrate the effectiveness of the base-isolation technique. Solving the problem with provided Julia codes is easy. The Julia codes can be effectively applied to solve a wider range of base-isolated structures to obtain the structural responses, thus the design for such a new kind of structures can be made easier.

Keywords: base isolation, base-isolated frame, nonlinear dynamic analysis, Julia.

Received: October 4th, 2017; revised: October 27th, 2017; accepted: November 2nd, 2017



1. Introduction

Over the years, many techniques have been developed to reduce or mitigate the vibration response in civil structures. These control techniques can be classified into four groups: passive, active, semi-active and hybrid. Active control systems require a power source for operation since electro-hydraulic actuators are used to provide control forces. This requirement faces to a risk when the power source is interrupted during storm or earthquake. Semi-active control systems offer a combination of features associated with passive and active control systems. They also consume energy to develop control forces whose magnitude is usually adjusted using a small power source. This technology of control is a promising one since semi-active control systems can produce a large control force at a significantly low power source like a battery. In hybrid control systems, a passive control device is used in combination with an active control actuator, but the two components do not function simultaneously. Instead, they are in active state in two different phases. Overall, three groups of control techniques presented above are of high technology and costly. In some situations, it is more reasonable to use one of the passive control techniques that do not require any power source to operate and are often much cheaper [1].

Seismic isolation is one of passive control techniques developed almost 100 years ago. Recently, this technique has become a practical strategy for earthquake-resistant design. In general, this technique uses isolators, or bearings, in the base of structures to endorse a surface of horizontal discontinuity. Base isolation techniques follow two basic approaches [2]. In the first approach, a layer of low lateral stiffness between the structure and the foundation is introduced. The natural periods of the whole system are lengthened to values much longer than that of fixed-base structure. Thus, the earthquake-induced forces in the superstructure are reduced. This type of isolation is effective even if the system is linear and undamped. The second most common type of isolation system uses sliding elements between foundation and base of the structure [3]. Therefore, the input energy from an earthquake is mainly converted into kinetic energy, and only a small amount of energy from earthquake transforms into the strain energy stored in the structure, allowing the structural elements to remain within an elastic range during earthquakes. The excellent performance of existing base-isolated structures during several past severe earthquakes proves that this control technique

¹ Dr, Faculty of Building and Industrial Construction, National University of Civil Engineering.

* Corresponding author. E-mail: thanhnx@nuce.edu.vn.

is reliable enough to protect structures from earthquakes, and their implementation will be promisingly more widespread in future. This article is limited to considering the dynamic behavior of structures using the isolation system in the first approach.

In the elastic design approach of base-isolated system, the design codes worldwide often assume no yielding in the superstructure and foundation. Eurocode (2004) allows a maximum behavior factor value of 1.5 for base-isolated buildings. US ASCE 7 (2010) allows the strength reduction factor for a base-isolated superstructure to be 0.375 times the one for a corresponding fixed-base structure and no larger than 2. Given that the large majority of ASCE 7 overstrength factors are between 2 and 3, the superstructure is likely to remain elastic for the design-level seismic hazard. In chapter 10 of Vietnamese code TCVN 9386:2012, the superstructures are also assumed to remain in elastic range during earthquakes. If the superstructure is assumed to be linear like this, and damping is viscous and classical, then the direct analysis or modal analysis of base-isolated structures are both acceptable. However, typically at least one of these assumptions is not valid.

Normally, the bearing systems behave inelastically. This nonlinear behavior is often captured by Bouc-Wen model [4-6]. Specifically, the Wen's model was used in [7] to optimize the performance of base-isolated system subjected to ground acceleration. Recently, Ghodke and Jangid [8] proposed a linear model of shape memory alloy to analyze base-isolated structures subjected to earthquake excitations. Previously, Jangid [9] investigated the response of a multi-story isolated structure mounted on lead rubber bearings subjected to seismic excitations. However, the detailed formulations were not shown in these researches. Also, in these researches, methods in the β -Newmark family were often used with very small time-steps (about 10^{-3} seconds) to attain acceptable accuracy. The methods proposed in [10] and [11] offered better numerical aspects in solving dynamic problems. So, in this article, we propose to use them for obtaining responses of base-isolated structures. In addition, the article also provides detailed formulation to solve the problems of base isolation using the well-known Runge-Kutta method. With these reformulations, accurate results can be achieved while the time-step size can be of larger values. The language used for modeling base-isolated structures is Julia. It is relatively new language, but its grammar is as simple as MATLAB and it often matches the performance of C language.



2. Modelling of base-isolated frames using linear elastic theory

2.1 Equivalent characteristics of base isolators

The characteristics of a seismic isolator (effective stiffness K_{eff} , and equivalent damping ratio ζ_{eq}) can be approximately extracted from data of cyclic loading experiment. For a single-degree-of-freedom (SDOF) oscillator, the effective stiffness K_{eff} is defined as:

$$K_{eff} = \frac{F_{max} - F_{min}}{u_{max} - u_{min}} \quad (1)$$

where F_{max} and F_{min} are maximum and minimum values of restoring forces, respectively; and u_{max} and u_{min} are maximum and minimum values of displacements, respectively. Those values can be determined from the experimental hysteretic loops (see Fig. 1). Recall that the energy dissipated by viscous damping in a cycle $u(t) = u_0 \sin \omega t$ is:

$$E_D = \int_0^{2\pi/\omega} F_D \dot{u} dt = \int_0^{2\pi/\omega} c \dot{u}^2 dt = \pi c \omega u_0^2 \quad (2)$$

Then, the damping ratio for the equivalent system ζ_{eq} is obtained by equating the true E_D^e of the bearing from experiment to the E_D of a viscously damped oscillator given in Eq. (2).

$$\zeta_{eff} = \frac{1}{2\pi} \frac{E_D^e \omega_n}{k u_0^2 \omega} \quad (3)$$

2.2 Modeling base-isolated frames

To make things simple, the behavior of isolation bearings is often modelled as a linear elastic element with viscous damping. The characteristics K_{eff} and ζ_{eq} of bearings are determined as mentioned above. Assume that the superstructure is also viscously damped linear elastic, then the equations of motion can be written as:

$$\mathbf{M}\ddot{\mathbf{U}} + \mathbf{C}\dot{\mathbf{U}} + \mathbf{K}\mathbf{U} = -\mathbf{M}\ddot{u}_g(t) \quad (4)$$



where: \mathbf{M} , \mathbf{C} and \mathbf{K} are the mass matrix, damping matrix, and stiffness matrix of the whole system, correspondingly; \mathbf{u} is the static influence coefficient vector; $\ddot{u}_g(t)$ is the ground acceleration. To make things even simpler, viscous damping is sometimes assumed to be of the classical type, or in other words, the product $\Phi^T \mathbf{C} \Phi$ is diagonal. The displacement, velocity and acceleration responses of the system \mathbf{U} , $\dot{\mathbf{U}}$ and $\ddot{\mathbf{U}}$ can be obtained by model analysis. However, more generally, the damping matrix is non-classical. It is normally due to the large difference between the damping property of the superstructure and the bearings. In this situation, the system of equations of motion is solved simultaneously to provide the responses \mathbf{U} , $\dot{\mathbf{U}}$ and $\ddot{\mathbf{U}}$. For this well-established problem, besides some well-known methods for solving these equations of motion, such as β -Newmark methods, θ -Wilson method, Houbolt method or some other finite difference ones, we can also use recently proposed methods that are more accurate and stable [10-12]. These methods are coded in Julia language as tools, provided in the package DirectStepIntegration.jl that can be downloaded and reused with the following Julia command:

```
Pkg.clone("https://github.com/tkris1004/DirectStepIntegration.git"); # clone the package
push!(LOAD_PATH,pwd()); # set the path
using DirectStepIntegration ; # declare to use the package
```

For more information on using these tools, refer to [11] or the coding of the package.

3. Modelling base-isolated frames using nonlinear theory

3.1 Bouc-Wen model of base isolators

Despite of the appeal of the very simplicity of the linear elastic theory in modeling the base-isolated structures, it is often not accurate. This flaw is due to the way it accounts for the damping in isolation system. The assumption that damping is viscous in the superstructure is acceptable (indeed, it is accepted in many design codes). However, the same assumption for the isolation system is not supported by many experiments that have demonstrated that the energy dissipated by rubber and rubber-like elastomeric materials is nearly rate-independent. Fig. 1 below shows typical experimental hysteresis loop of different isolation bearings.

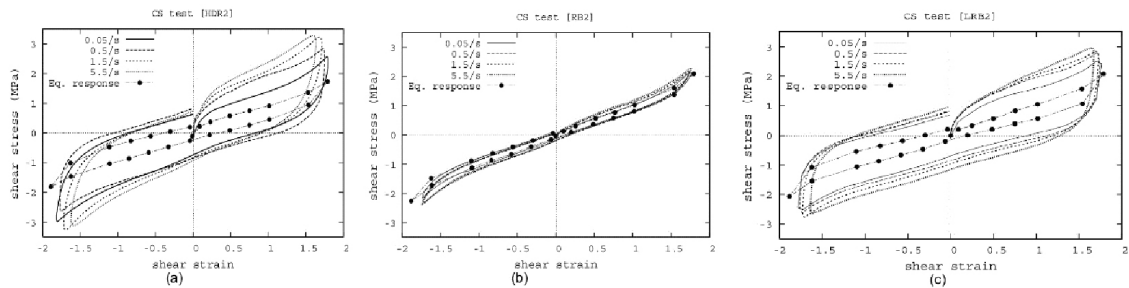


Figure 1. Typical hysteresis loop of different isolation bearings (adapted from [13])

Eq. (2) shows that E_D is a function of forcing frequency ω . Experiments have shown that E_D is nearly frequency-independent. This kind of damping is also called “hysteresis damping”, or “rate-independent damping”. A well accepted analytical model to capture this behavior of bearings is Bouc-Wen model. This model can capture, in analytical form, a range of hysteretic cycle shapes matching the behavior of a wide class of hysteretic systems. Due to its versatility and mathematical tractability, the Bouc-Wen model has gained popularity. It has been extended and applied to a wide variety of engineering problems. In the field of structural control, the Bouc-Wen model has been used in the modeling of behavior of magneto-rheological dampers, base-isolation devices for buildings and other kinds of damping devices as well.

According to the Bouc-Wen model, the restoring force restoring force can be visualized as two springs connected in parallel and is given by the following expression:

$$F(u_b(t), z(t), t) = \alpha k_e u_b(t) + (1 - \alpha) k_e u_y z(t) \quad (5)$$

where: $\alpha = k_p/k_e$ is the ratio of post-yield stiffness k_p to pre-yield (elastic) stiffness k_e of the base isolators; u_y is the yield displacement; $z(t)$ is non-observable hysteretic displacement which is given by the following differential equation with initial condition $z(0)=0$:

$$u_y \dot{z}(t) = A \dot{u}_b(t) - \beta |\dot{u}_b(t)| |z(t)|^{m-1} z(t) - \gamma \dot{u}_b(t) |z(t)|^n \quad (6)$$

In the above equation, $A, \beta > 0, \gamma$, and n are dimensionless parameters controlling the behavior of the model. The parameter n control how sharp the transition from elastic to inelastic is. For small values of the positive exponential parameter n , this transition is smooth, while for large values this transition is abrupt. Parameters A, β and γ control the size and shape of the loop. Normally, A is set to unit to remove the redundancy among these parameters. The valid range of γ is found to be $[-\beta, \beta]$.

3.2 Modeling base-isolated frames

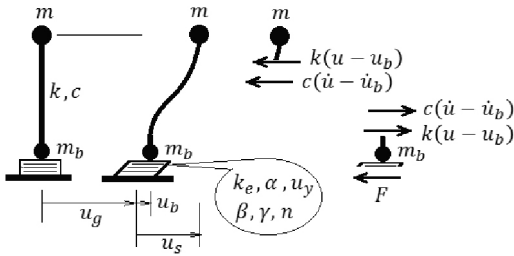


Figure 2. A 2-DOF model of a base-isolated structure

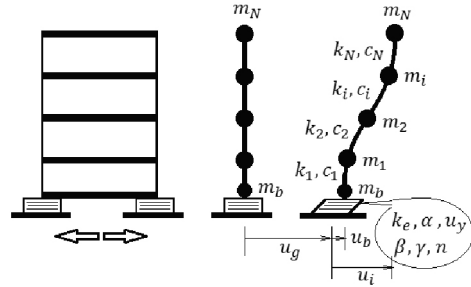


Figure 3. A base isolation embedded under a (cantilever) structure with N-DOFs

Fig. 2 shows a simplified model of a 2-DOF base-isolated structure. Top mass equilibrium gives:

$$m\ddot{u}_s + c(\dot{u}_s - \dot{u}_b) + k(u_s - u_b) = -m\ddot{u}_g \tag{7}$$

Equilibrium of the bottom mass gives:

$$m_b\ddot{u}_b + F - c(\dot{u}_s - \dot{u}_b) - k(u_s - u_b) = -m_b\ddot{u}_g \tag{8}$$

Substituting F from Eq. (5) into this equation yields:

$$m_b\ddot{u}_b + \alpha k_e u_b(t) + (1 - \alpha)k_e u_y z(t) - c(\dot{u}_s - \dot{u}_b) - k(u_s - u_b) = -m_b\ddot{u}_g \tag{9}$$

Eqs. (6), (7) and (9) fully describe the whole system. This set of equations can be solved using simple numerical methods, such as the central difference method, or the methods in the β -Newmark family. However, we also have very powerful tools in Julia language to deal with this kind of problem. We recommend using these tools over other methods because these tools can solve much more complicated problems. To solve the set of equations (6), (7) and (9) with Julia, we need to cast them in a state-space formulation. The state vector is:

$$\mathbf{y} = [y_1 \ y_2 \ y_3 \ y_4 \ y_5]^T = [u_s \ u_b \ \dot{u}_s \ \dot{u}_b \ z]^T \tag{10}$$

Then:

$$\dot{\mathbf{y}}(t) = \begin{bmatrix} \dot{y}_1 \\ \dot{y}_2 \\ \dot{y}_3 \\ \dot{y}_4 \\ \dot{y}_5 \end{bmatrix} = \begin{bmatrix} \dot{u}_s \\ \dot{u}_b \\ \ddot{u}_s \\ \ddot{u}_b \\ \dot{z} \end{bmatrix} = \begin{bmatrix} y_3 \\ y_4 \\ -\frac{1}{m} [c(y_3 - y_4) + k(y_1 - y_2)] - \ddot{u}_g \\ -\frac{1}{m_b} [\alpha k_e y_2 + (1 - \alpha)k_e u_y y_5 - c(y_3 - y_4) - k(y_1 - y_2)] - \ddot{u}_g \\ \frac{1}{u_y} [y_4 - \beta |y_4| |y_5|^{n-1} y_5 - \gamma y_4 |y_5|^n] \end{bmatrix} \tag{11}$$

There are several good methods for solving this equation among which the Runge-Kutta method is commonly used due to its superiority performance. This method is also employed in this article using a Julia package named DifferentialEquation.jl contributed by Rackauckas [14].

In case of multi-degree-of-freedom (MDOF) system, such as the case of multi-story building shear frames, the state-space formulation needs a little arrangement. The model for the superstructure is assumed to be a cantilever with N concentrated masses attached at floor levels as shown in Fig. 3. Denote the mass matrix, damping matrix, and stiffness matrix of the fixed-base structure as $\mathbf{M}_s, \mathbf{C}_s$ and \mathbf{K}_s , respectively. Like Eq. (7), equilibrium of the superstructure can be written as:

$$\mathbf{M}_s \ddot{\mathbf{U}}_s + \mathbf{C}_s (\dot{\mathbf{U}}_s - \dot{\mathbf{u}}_b) + \mathbf{K}_s (\mathbf{U}_s - \mathbf{u}_b) = -\mathbf{M}_s \ddot{\mathbf{u}}_g \tag{12}$$



where: $\mathbf{U}_s = [u_1 \ u_2 \ \dots \ u_N]^T$ is the displacement vector of the superstructure with respect to the foundation (bottom layer of the base isolator). The influence vector $\mathbf{1}$ for the case of shear frames is unit vector, $\mathbf{1} = [(1 \ 1 \ \dots \ 1)]^T$. Equilibrium of the mass m_b gives:

$$m_b \ddot{u}_b + F - c_1 (\dot{u}_1 - \dot{u}_b) - k_1 (u_1 - u_b) = -m_b \ddot{u}_g \tag{13}$$

Considering that $u_1 = \delta_1 \mathbf{U}_s$ where $\delta_1 = \begin{bmatrix} 1 & 0 & \dots & 0 \\ \underbrace{\hspace{2cm}}_{N \text{ components}} \end{bmatrix}$, Eq. (13) can be rewritten as:

$$m_b \ddot{u}_b + \alpha k_e u_b(t) + (1 - \alpha) k_e u_y z(t) - c_1 (\delta_1 \dot{\mathbf{U}}_s - \dot{u}_b) - k_1 (\delta_1 \mathbf{U}_s - u_b) = -m_b \ddot{u}_g \tag{14}$$

Now, we will write Eqs. (6), (12), and (14) in state-space form as:

$$\dot{\mathbf{y}}(t) = \begin{bmatrix} \dot{\mathbf{U}}_s \\ \dot{u}_b \\ \ddot{\mathbf{U}}_s \\ u_b \\ \dot{z} \end{bmatrix} = \begin{bmatrix} y_3 \\ y_4 \\ -\mathbf{M}_s^{-1} [\mathbf{C}_s (y_3 - \mathbf{y}_4) + \mathbf{K}_s (y_1 - \mathbf{y}_2)] - \mathbf{1} \ddot{u}_g \\ -\frac{1}{m_b} [\alpha k_e y_2 + (1 - \alpha) k_e u_y y_5 - c_1 (\delta_1 y_3 - y_4) - k_1 (\delta_1 y_1 - y_2)] - \ddot{u}_g \\ \frac{1}{u_y} [y_4 - \beta |y_4| |y_5|^{n-1} y_5 - \gamma y_4 |y_5|^n] \end{bmatrix} \tag{15}$$

where: $\mathbf{y}(t) = [y_1 \ y_2 \ y_3 \ y_4 \ y_5]^T = [\mathbf{U}_s \ u_b \ \dot{\mathbf{U}}_s \ \dot{u}_b \ z]^T$ is the state vector.

4. Nonlinear responses of base-isolated frames - case studies

4.1 Base-isolated shear frame with non-classical damping

Consider a shear frame, initially at rest, modeled as 4-DOF system as shown in Fig. 3, with floor masses $m_s = 10 \text{ kN.s}^2/\text{m}$. The lateral stiffness of each story is $k_s = 1.6 \times 10^4 \text{ kN/m}$. We consider this frame in two situations. For fixed-base situation, the mass matrix, stiffness matrix and damping matrix are:

$$\mathbf{M}_s = m_s \begin{bmatrix} 1 & & & \\ & 1 & & \\ & & 1 & \\ & & & 1 \end{bmatrix}; \quad \mathbf{K}_s = k_s \begin{bmatrix} 2 & -1 & 0 & 0 \\ & 2 & -1 & 0 \\ & & 2 & -1 \\ \text{symm.} & & & 1 \end{bmatrix}; \tag{16}$$

The damping of the frame is assumed to be viscous and proportional to the stiffness matrix $\mathbf{C} = a_1 \mathbf{K}$ where $a_1 = 0.0025$ (classical damping, following one of the Rayleigh models). From this, we have:

$$\mathbf{C}_s = c_s \begin{bmatrix} 2 & -1 & 0 & 0 \\ & 2 & -1 & 0 \\ & & 2 & -1 \\ \text{symm.} & & & 1 \end{bmatrix}; \quad \text{with } c_s = 40 \text{ kN.s/m} \tag{17}$$

For the base-isolated situation, the properties of the bearing are given as:

$$m_b = m_s; \quad k_b = k_s / 2; \quad c_b = 1.5 c_s \tag{18}$$

Thus, the augmented structural matrices now are:

$$\mathbf{M} = \begin{bmatrix} m_b & 0 \\ 0 & \mathbf{M}_s \end{bmatrix}; \quad \mathbf{K} = \begin{bmatrix} k_s + k_b & \mathbf{k}_{sb} \\ \mathbf{k}_{sb}^T & \mathbf{K}_s \end{bmatrix}; \quad \mathbf{C} = \begin{bmatrix} c_s + c_b & \mathbf{c}_{sb} \\ \mathbf{c}_{sb}^T & \mathbf{C}_s \end{bmatrix} \tag{19}$$

where: \mathbf{k}_{sb} and \mathbf{c}_{sb} are coupling matrices that can be found as:

$$\mathbf{k}_{sb} = [-k_s \ 0 \ 0 \ 0]; \quad \text{and } \mathbf{c}_{sb} = [-c_s \ 0 \ 0 \ 0] \tag{20}$$

The non-classical damping property of the whole system can be verified by $\phi_n^T \mathbf{C} \phi_n \neq 0$ for any $n \neq r$, where ϕ_n is the n th mode shape of the augmented system. The frame is subjected to the El Centro 1940 earthquake with acceleration record of the ground given in the Appendix of Chapter 6 in [3]. The equation of motion is shown in Eq. (4), where the influence vector is $\mathbf{1} = [1 \ 1 \ 1 \ 1]^T$ for the case of fixed-base, or $\mathbf{1} = [(1 \ 1 \ \dots \ 1)]_{1 \times 5}^T$ for the case of base-isolation. Similarly, different displacement vector is defined for the two cases: $\mathbf{U} = [u_1 \ u_2 \ u_3 \ u_4]^T$ for the first case, and $\mathbf{U} = [u_b \ u_1 \ u_2 \ u_3 \ u_4]^T$ for the second case.

We would like to consider the responses of this system under these two cases and compare them. This problem can be solved using tools in DirectStepIntegration.jl package or using Runge-Kutta method in built-in commands in Julia. In this example, we will use tools in package DirectStepIntegration.jl (refer also to Section 3.1). After initiating the package, the rest of Julia codes is as follows:

```

m_s = 10; c_s = 40; k_s = 1.6e4; m_b = 10; c_b = 60; k_b = 1.6e3;
c_sb = [-c_s 0 0 0]; k_sb = [-k_s 0 0 0]; M_fb = eye(4)*m_s; M_bi = eye(5)*m_s;
C_fb = c_s*[2 -1 0 0; -1 2 -1 0; 0 -1 2 -1; 0 0 -1 1]; C_bi = [c_s+c_b c_sb; c_sb' C_fb];
K_fb = k_s*[2 -1 0 0; -1 2 -1 0; 0 -1 2 -1; 0 0 -1 1]; K_bi = [k_s+k_b k_sb; k_sb' K_fb];
dth_fb = (M_fb, C_fb, K_fb); dth_bi = (M_bi, C_bi, K_bi); tz_fb = (0.02, 2000); tz_bi = (0.02, 2000);
ic_fb = ([0.; 0.; 0.; 0.], [0.; 0.; 0.; 0.]); ic_bi = ([0.; 0.; 0.; 0.], [0.; 0.; 0.; 0.]);
p_fb = (0.02, -(readdlm("ElCentro.txt")[ :, 1])*ones(1,4)*M_fb);
p_bi = (0.02, -(readdlm("ElCentro.txt")[ :, 1])*ones(1,5)*M_bi);
u_fb, ud_fb, u2d_fb=tkris5(dth_fb, tz_fb, ic_fb, p_fb);
u_bi, ud_bi, u2d_bi=tkris5(dth_bi, tz_bi, ic_bi, p_bi);

```

The maximum value of the top displacement $\max_t |u_{top}(t)| = 8.258E-2$ m of fixed-base structure is much larger than that of base-isolated structure $\max_t |u_{top}(t)| = 1.670E-2$ m. Similarly, for the top total acceleration, $\max_t |\ddot{u}'_{top}(t)| = 15.05$ m/s² of fixed-base structure is much larger than $\max_t |\ddot{u}'_{top}(t)| = 2.89$ m/s² of base-isolated one. The total acceleration is defined as $\ddot{u}'(t) = \ddot{u}(t) + \ddot{u}'_g(t)$. Table 1 shows the top displacement and acceleration for the first five steps. The responses over the time from 0 to 40 seconds are shown in Fig. 4 where we can see the effectiveness of the base isolation in reducing the responses.

Table 1. Responses of the system for the first five steps

t (seconds)	u_{top} (m)		\ddot{u}'_{top} (m/s ²)	
	Fixed-base	Base-isolated	Fixed-base	Base-isolated
0.02	9.245E-6	3.191E-7	-1.101E-1	-1.101E-1
0.04	5.567E-5	3.917E-6	-7.131E-3	-7.132E-3
0.06	1.428E-4	1.524E-5	-1.313E-2	-1.326E-2
0.08	2.661E-4	3.689E-5	-9.164E-3	-7.241E-3
0.1	4.238E-4	7.015E-5	-3.767E-2	-2.633E-2

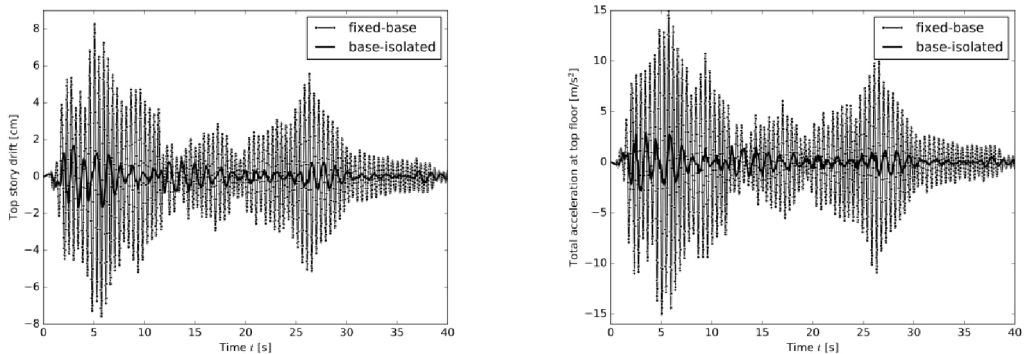


Figure 4. Responses of the system during the first forty seconds

4.2 MDOF (4-storey) shear frame with damping modeled as Bouc-Wen element

The isolation system is a lead-rubber-bearing, modelled as a Bouc-Wen element with the following values of parameters: $m_b=10$ tons, $u_y=5$ mm, $k_g=8$ kN/mm, $\alpha=0.1$, $n=2$, $\beta=0.9$ and $\gamma=0.1$. The same super-structure and the same (seismic) loading condition are used in this case study as in the previous case study in Section 4.1. For fixed-base situation, the mass matrix, stiffness matrix and damping matrix are given in Eqs. (16) and (17). The following Julia codes are used to obtain the system responses.



```

m_s = 10000; c_s = 0.04*m_s*100; k_s = 1600*m_s; m_b = 10000;
M = eye(4)*m_s; C = c_s*[2 -1 0 0; -1 2 -1 0; 0 -1 2 -1; 0 0 -1 1]; K = k_s*[2 -1 0 0; -1 2 -1 0; 0 -1 2 -1; 0 0 -1 1];
dth = (M, C, K); tz = (0.02, 2000); ic = [0.; 0.; 0.; 0.; 0.; 0.; 0.; 0.; 0.; 0.];
ztn_raw = (0.02, readlm("ElCentro.txt")[:, 1]);
alp=0.1; beta1=0.9; gamm=0.1; n=2; uy=0.005; ke=k_s/2;
ccd = (alp, beta1, gamm, n, uy, ke); rk_bi(dth, ccd, tz, ic, ztn_raw);
    
```

Results obtained after running these lines of Julia code are shown below. The ground acceleration \ddot{u}_g input to the frame, the dimensionless hysteretic parameter z , the bearing displacement u_b , the restoring force on the bearing F , the top story drift u_{top} in base-isolated frame and in fixed-base frame are shown in Table 2 for the first five steps. Table 2 also provides maximum of selected responses. From this table, the effectiveness of the bearing system in reducing the structural responses can be seen. We can also see that during the first 0.1 seconds, there is no reduction in the top story drift contributed by the isolation system. This is certainly due to the hysteresis phenomenon of the bearing.

Table 2. Responses of the system for the first five steps

t (s)	\ddot{u}_g (m/s ²)	z	F (kN)	u_b (m)	u_{top} (m)	
					Base-isolated	Fixed-base
0.02	-1.427E-2	7.291E-11	1.167E-5	1.458E-8	1.197E-5	9.245E-6
0.04	-1.101E-1	1.066E-8	1.795E-3	2.131E-6	6.456E-5	5.567E-5
0.06	-1.030E-1	3.734E-7	5.976E-2	7.468E-5	1.584E-4	1.428E-4
0.08	-8.973E-2	2.749E-6	4.400E-1	5.499E-4	2.887E-4	2.661E-4
0.1	-9.687E-2	1.059E-5	1.696E+0	2.119E-3	4.579E-4	4.238E-4
Maximum values over 40 seconds				6.013E-2	1.302E-2	8.258E-2

In Fig. 5, beside the ground acceleration record, the relative bearing displacement and the story drift of the top floor are shown. The comparison in Fig. 6(a) shows that there is a big reduction in the top story drift when the frame is base-isolated. We can also observe similar reduction in other response quantities of the base-isolated frame as well. Due to limited number of pages for this article, we do not show all the results here, but readers can verify by themselves. The hysteretic behavior of the bearing can be seen through the loops in Fig. 6(b).

5. Conclusions

This article introduced the ways to model base-isolated frames using both linear elastic theory

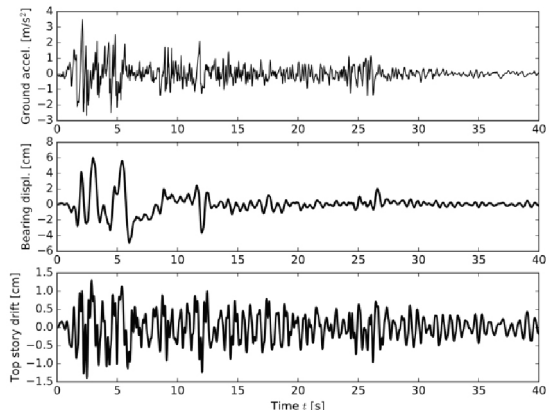


Figure 5. Ground acceleration and responses of the system during the first forty seconds

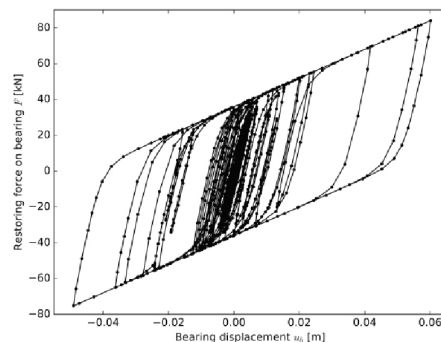
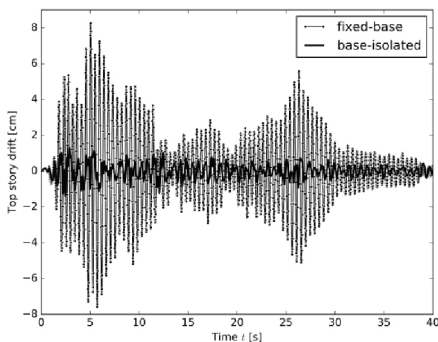


Figure 6. (a) Comparison of top story drift; (b) Hysteretic loops

and nonlinear theory. In both cases, the nonlinear dynamic responses of the whole system can be obtained from commands of Julia programming language without much difficulty. The effectiveness of isolation system is illustrated through some case studies. Further studies can be dealt with the influence of bearing parameters to system responses, the optimization of these parameters to obtain optimum design of frames subjected to time-varying loading conditions, such as wind loads and/or earthquake-induced loads.

The author gratefully acknowledges the partial support of this work by the (Vietnam) National University of Civil Engineering (NUCE) under grant 145-2017/KHXD-TĐ. Personal communication with Chris Rackauckas is also useful as when I used his DifferentialEquation.jl package in my code thus it is acknowledged here.

References

1. Housner G., Bergman L. A., Caughey T. K., Chassiakos A. G., Claus R. O., Masri S. F., and Yao J. T. (1997), "Structural control: past, present, and future," *Journal of engineering mechanics*, 123(9):897-971.
2. Saaed T. E., Nikolakopoulos G., Jonasson J.-E., and Hedlund H. (2015), "A state-of-the-art review of structural control systems," *Journal of Vibration and Control*, 21(5):919-937.
3. Chopra A.K. (2012), *Dynamics of structures (Theory and applications to earthquake engineering)*, 4th ed., Prentice Hall.
4. Wikipedia Foundation Inc. (2017). Available: https://en.wikipedia.org/wiki/Bouc%E2%80%93Wen_model_of_hysteresis. [Accessed 16 September 2017].
5. Kelly J. (1986), "A seismic base isolation: review and bibliography," *Soil Dyn Earthq Eng*, 5(3):202-216.
6. Naeim F., and Kelly J. M. (1999), *Design of seismic isolated structures: from theory to practice*, Wiley.
7. Constantinou M. C., and Tadjbakhsh I. G. (1985), "Hysteretic dampers in base isolation: random approach," *Journal of Structural Engineering*, 111(4):705-721.
8. Ghodke S., and Jangid R. (2016), "Equivalent linear elastic-viscous model of shape memory alloy for isolated structures," *Advances in Engineering Software*, 99:1-8.
9. Jangid R. (2007), "Optimum lead-rubber isolation bearings for near-fault motions," *Engineering structures*, 29(10):2503-2513.
10. Thanh N.X. (2013), "A new time integration scheme for dynamic analysis of structures," in *Proceedings of the 11th National Conference on Mechanics of Solid Bodies*, Ho-Chi-Minh City, 2:1064-1072.
11. Thanh N.X., "Improved time step integration methods in dynamic analysis of MDOF structures", *Journal of Science and Technology in Civil Engineering*, 11(5):40-48.
12. Razavi S., Abolmaali A., and Ghassemieh M. (2007), "A Weighted Residual Parabolic Acceleration Time Integration Method for Problems in Structural Dynamics," *Computational Methods in Applied Mathematics*, 7(3):227-238.
13. Bhuiyan A., and Okui Y. (2012), "Mechanical Characterization of Laminated Rubber Bearings and Their Modeling Approach," Chapter in book *Earthquake Engineering*, Halil Sezen (Ed.), DOI: 10.5772/50405.
14. Rackauckas C. (2017), Available: <https://github.com/JuliaDiffEq/DifferentialEquations.jl>. [Accessed 3 October 2017].
15. Wikipedia Foundation Inc. (2017), Available: https://en.wikipedia.org/wiki/Base_isolation. [Accessed 14 September 2017].
16. Kelly J., Leitmann G., and Soldatos A. (1987), "Robust control of base-isolated structures under earthquake excitation," *Journal of Optimization Theory and Applications*, 53(2):159-180.